Spin–orbit interaction in the photoemission spectra of noble metal surface states

Spin–orbit interaction in the photoemission spectra of noble metal surface states

Friedrich Reinert

Universität des Saarlandes, Fachrichtung 7.2—Experimentalphysik, D-66041 Saarbrücken, Germany

E-mail: friedel@mx.uni-saarland.de

Abstract
By use of photoemission spectroscopy with high resolution in both energy and momentum, one is able to observe a considerable splitting of the Shockley-type surface state on the (111)-face of gold. This splitting exists over the complete two-dimensional Fermi surface of this surface state but disappears at normal emission. A comparison with fully relativistic density functional calculations proves that the splitting is caused by spin–orbit interaction, which—in combination with the lack of inversion symmetry at the surface—resolves the spin degeneracy of the surface state band. This paper gives a summary of recent experimental and theoretical investigations on the split Shockley state on Au(111). In addition, it will be demonstrated that the splitting is influenced by adsorbates, and it will be discussed why it has not been observed experimentally on other noble metals.

1. Introduction

1.1. Surface states in general

The approach to the theoretical description of solids starts with an infinite crystal with a perfect translational symmetry, where the ions are arranged in a regular periodic array. But such a perfect crystal is fictitious; in every real crystal there must exist distortions of the periodicity of the lattice, imperfections, that are important for many physical properties of the solid. The most obvious of these imperfections is the *crystal surface* which forms the region of contact with the surroundings. Here one can observe completely new phenomena and physical features, e.g. particular surface phonon modes or the electronic surface states.

Specific electronic states localized near the crystal boundary were predicted theoretically as early as 1932 by Tamm [1]. An important step in the understanding of these surface states was made a few years later by Shockley [2], who investigated theoretically, how surface states originate from the discrete levels of atoms. To commemorate these fundamental works today,

one distinguishes between two different kinds of surface state: *Tamm states*, which are split off from weakly hybridized bulk states due to the change of the potential in the outermost cells, and *Shockley states*, which are caused by a symmetric termination of the periodic potential in systems where the atomic orbitals overlap sufficiently that band crossing can occur. The present paper deals with the second type, in particular Shockley states on the (111)-faces of noble metals.

In general, calculations of the electronic band structure are based on the *one-electron approximation*, i.e. one electron is embedded in the periodic ionic potential plus an averaged constant field of all other electrons, which replaces the individual pair potentials. In addition, one neglects nuclear motions and assumes fixed ionic potentials centred at the periodic lattice of the crystal (*Born–Oppenheimer approximation*). The solution of such a one-electron Schrödinger equation gives the well known Bloch electrons, travelling independently throughout the crystal with a real crystal momentum $p = \hbar k$. If the crystal is terminated by a surface, the wavevector k may also assume complex values and one gets energy eigenvalues that lie inside the energy gaps of the infinite crystal. Due to the imaginary part of of the wavevector component perpendicular to the surface $k_\perp$, these new states are monotonically damped in the direction of the vacuum and also damped, but still oscillating, inside the crystal. Consequently, these states are *localized* to the crystal surface [3]. Therefore, surface states play an important role for the dynamics of surface or interface related processes, such as adsorption, catalysis and, therewith, chemical reactions at surfaces [4].

Since the first experimental observation of surface states on noble metals in the 1970s [5, 6], there has been a continuous interest on the spectroscopic investigation of these states [7–10], both on clean and adsorbate covered surfaces. Besides their implications for chemical surface reactions, metallic surface states are fundamental model systems for the understanding of many-body effects, e.g. electron–electron and electron–phonon interaction [9, 11–18]. For experimental reasons, the confinement to the surface and the resulting two-dimensionality make them ideally suitable for the investigation by high-resolution photoemission in the VUV range.

A comparatively new experimental method for the investigation of surface states is spectroscopy with a surface tunnelling microscope (STMS) by measuring the differential tunnelling current $\mathrm{d}I/\mathrm{d}V$ [19–22]. It was demonstrated that from these measurements one is able to determine the intrinsic lifetime width of Shockley states at the band minimum in excellent agreement with results from photoemission experiments [23] and inelastic lifetime calculations [24]. Furthermore, a detailed analysis of the energy dependent spatial distribution of the tunnelling current can give information about the surface state dispersion—both below and above the Fermi level—and the topology of the Fermi surface [19, 25, 26].

1.2. Experimental principles

Photoemission spectroscopy is a surface sensitive technique and is therefore an important experimental method to study the surface electronic properties of solids [27]. The method is based on the photoelectric effect: photons are impinging on a sample and are able to excite electrons out of the surface, if their energy is large enough to exceed the work function Φ_0 of the surface. In the one-electron picture, this condition of energy conservation is expressed by

$$E_{kin} = h\nu - E_B - \Phi_0, \tag{1}$$

where E_B is the binding energy of the electron in the ground state relative to the Fermi level. E_{kin} describes the kinetic energy of the excited photoelectron in the vacuum, which can be measured by the photoelectron analyser. In addition, the emission angle θ of the

detected photoelectron can be used to calculate the parallel—i.e. the in-plane—component $\boldsymbol{k}_\parallel = (k_x, k_y)$ of the crystal wave vector $\boldsymbol{k} = (k_\perp, \boldsymbol{k}_\parallel)$ of the Bloch state by

$$|\boldsymbol{k}_\parallel| = \frac{\sqrt{2m_e}}{\hbar} \sqrt{E_{kin}} \sin\theta. \tag{2}$$

Since the surface states are two dimensional, the parallel component $\boldsymbol{k}_\parallel$ sufficiently determines the wavevector of the involved one-electron state. The energy–momentum relation $E_B(\boldsymbol{k}_\parallel)$ (for simplicity, the index B will be suppressed in the following), resulting from the combination of equations (1) and (2), defines the dispersion of the surface state, and with that also its two-dimensional *Fermi surface*.

In addition to the one-electron properties described above, photoemission gives information about the *line-shape* of the surface state, which reflects the many-body scattering processes in the system. The excited quasi-particle state, consisting of a photo-hole in the solid and the out-going photoelectron, has a finite lifetime due to scattering with phonons, lattice imperfections or other electrons. In the simplest picture, this finite lifetime leads in the photoemission spectra to a *Lorentzian* with a full width at half maximum Γ which is defined by the lifetime τ of the photo-hole: $\Gamma = \hbar/\tau$. Γ gives the intrinsic lifetime width and is a sum of the contributions from the different scattering processes described above:

$$\Gamma = \Gamma_{el-el} + \Gamma_{el-ph} + \Gamma_{el-imp}. \tag{3}$$

For the analysis of the intrinsic linewidth and line-shape in experimental data one has to consider additional broadening effects which are due to a finite energy or angular resolution of the measurement. More about the photoemission line-shape of surface states can be found for example in [7, 9, 10, 23].

1.3. Spin–orbit splitting of a surface state

1.3.1. History. The first experimental proof of a split Shockley state by photoemission spectroscopy was published by LaShell *et al* [28]. They investigated an Au(111) surface at room temperature and used a photon energy of $h\nu = 11.83$ eV (Ar I), which—in comparison to the more common He I or He II energies—has the advantage of a significantly better k-resolution (cf equation (2)). Off normal emission, i.e. at $k_\parallel > 0$, their photoemission spectra showed a line doublet with an energy difference that increases linearly with $k_\parallel$. They interpreted the origin of the splitting correctly as spin–orbit coupling of the sp-like surface state electrons. However, because these results have not been reproduced over several years and, furthermore, the splitting has not been observed in spectroscopic investigations by use of an STMS, there was a discussion of possible other reasons in the literature [29–31]. In particular, it was discussed whether the peculiar herringbone reconstruction of the Au(111) surface—the herringbone pattern originates from adjacent domains of a $22 \times \sqrt{3}$ reconstruction [32]—might have an influence on the spectroscopic results on the Shockley state. The (111)-faces of other noble metals do neither show this reconstruction nor has a splitting of the surface state been observed. But meanwhile, all uncertainties are removed and the results by LaShell *et al* [28] are theoretically and experimentally corroborated [33, 34].

1.3.2. Theory. The following section gives a sketch of the theoretical idea for the explanation of the spin–orbit splitting, as suggested by LaShell *et al* [28] and elaborated in more detail by Petersen and Hedegård [33]. In the one-electron approximation the spin–orbit interaction of an electron in the potential $V(\boldsymbol{r})$ of the solid is described by the coupling term

$$H_{SOC} = \frac{\hbar^2}{4\mathrm{i}m^2c^2} \boldsymbol{\sigma} \cdot (\boldsymbol{\nabla}V \times \boldsymbol{\nabla}), \tag{4}$$

with Pauli spin operator $\boldsymbol{\sigma}$ working on the spin component of the spinors $\psi(\boldsymbol{r}, s)$, the gradient in the parentheses on the space component. If there is no external magnetic field, this term is the only necessary relativistic correction in the considered context. For a spherically symmetric potential we have $\nabla V = (\boldsymbol{r}/r) \mathrm{d}V/\mathrm{d}r$ and the coupling term can be written as

$$H_{SOC} = \frac{1}{2m^2 c^2} \frac{1}{r} \frac{\mathrm{d}V}{\mathrm{d}r} (\boldsymbol{s} \cdot \boldsymbol{l}), \tag{5}$$

with the spin operator $\boldsymbol{s} = \frac{1}{2}\hbar\boldsymbol{\sigma}$ and the operator for the orbital angular momentum $\boldsymbol{l} = \boldsymbol{r} \times \boldsymbol{p} = -\mathrm{i}\hbar\boldsymbol{r} \times \nabla$, which finally explains the name of the interaction.

The *Kramers degeneracy* between $\psi_k(\boldsymbol{r}, s)$ and its complex conjugate $\psi_k^*(\boldsymbol{r}, s)$ (i.e. reversed momentum and spin), which is a result of the fundamental principle of *time reversal symmetry*, remains unaffected by H_{SOC}. Therefore one gets $E(\boldsymbol{k}, \uparrow) = E(-\boldsymbol{k}, \downarrow)$. If the crystal potential has a centre of inversion (i.e. $\psi_k(\boldsymbol{r}, s) = \psi_k(-\boldsymbol{r}, s)$) one gets $E(\boldsymbol{k}, \uparrow) = E(-\boldsymbol{k}, \uparrow)$. The combination of these two conditions results in $E(\boldsymbol{k}, \uparrow) = E(\boldsymbol{k}, \downarrow)$; in other words, there is no energy splitting depending on the electron spin. This means that noble metals, which crystallize in the fcc structure, do not have a spin–orbit split bulk band structure.

The surface destroys the inversion symmetry in the direction of the surface normal and the spin degeneracy might be resolved. A qualitative description of the resulting surface state structure can be given by a nearly free electron (NFE) model, which is the simplest ansatz to describe a surface state. Here, we only consider the component of the potential gradient perpendicular to the surface, i.e. $\nabla V = \mathrm{d}V/\mathrm{d}x \, \boldsymbol{e}_x$. $\boldsymbol{e}_x$ is the unit vector perpendicular to the surface. The k-vector of a surface state is parallel to the surface and thus perpendicular to ∇V. The vector in the parentheses of equation (5) $(\nabla V \times \nabla) = -\mathrm{i}\hbar(\nabla V \times \boldsymbol{p})$ lies also in the surface and is always perpendicular to $\boldsymbol{p} = \hbar\boldsymbol{k}$, and the size of the splitting is proportional to $|\boldsymbol{k}_\parallel|$. The NFE model is not suitable to give usable quantitative results, because the core region of the ionic potential, where the gradient of the potential is large, is neglected. The NFE energy splitting at the Fermi level is of the order of only 10^{-3} meV, five orders of magnitude below the experimental value. As discussed later, appropriate quantitative results can be obtained from *ab initio* slab layer calculations. However, the NFE is able to describe the nature of the splitting correctly.

The result can be illustrated at the Fermi surface topology as given in figure 1. One gets two concentric circular Fermi surfaces with opposite spin orientations, remaining perpendicular to $\boldsymbol{k}_F$ for all points on the Fermi surface. Note that the distribution of the spins is completely symmetric and therefore the net spin of the surface state is equal to zero: of course, there is no surface magnetism due to the split Shockley state on Au(111).

2. Experimental setup and sample preparation

The experiments presented here have been performed with a Scienta SES200 photoemission spectrometer, equipped with a microwave-driven monochromatized VUV lamp and an open-cycle cryostat manipulator. The photon energy was $h\nu = 21.23$ eV (He I$_\alpha$) and the sample temperature was set to constant $T = 30$ K. For the temperature dependence of surface states see for example [11, 12, 35]. The base pressure of the UHV system was typically below 5×10^{-11} mbar, increasing to approximately 1×10^{-9} mbar during the measurement, caused by the He leakage from the differentially pumped VUV lamp.

The spectrometer allows us to measure an angular range of $\pm 7°$ simultaneously, equivalent to a $\bar{\Gamma}$-centred cut through the surface Brillouin zone (SBZ) within $k_\parallel = \pm 0.26$ Å^{-1} at He I$_\alpha$ radiation. This range is large enough to map the whole occupied surface state band
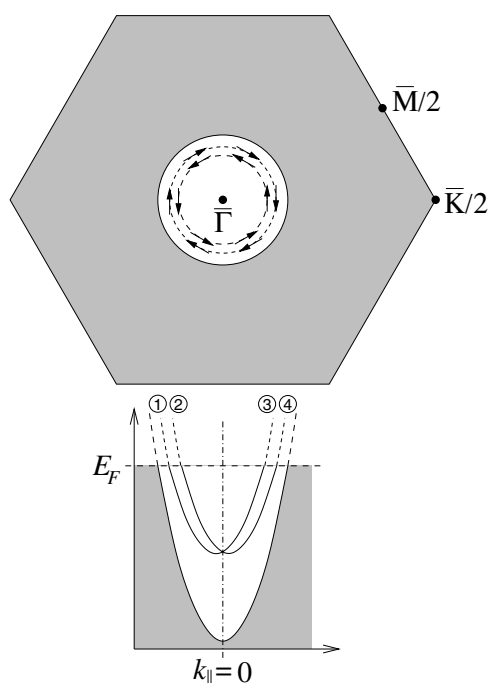
Figure 1. Upper panel, section of the SBZ of the unreconstructed Au(111) surface. The $\bar{\Gamma}\bar{K}$ distance is $\pi\sqrt{32}/3a = 1.45$ Å^{-1}. Lower panel, schematic view of the split surface state dispersion in a cut through $\bar{\Gamma}$.

of the systems investigated here. The energy resolution in this angular resolved mode was $\Delta E = 3.5$ meV, the angular resolution $\Delta\theta \lesssim \pm 0.15°$. Typical accumulation times for one complete data set, as for example given in figure 2, are 8 min or less. To map the complete two-dimensional Fermi surface it is necessary to use the rotational degree of freedom of the manipulator. The rotation axis lies in the surface plane, parallel to the entrance slit of the analyser.

The surfaces of the polished single crystals have been prepared by the standard *in situ* sputtering/annealing cycles as described in the literature [36]. The last preparational step is an annealing to temperatures close to 700 °C for a few minutes. Since time dependent changes of the PE spectra indicate a fast surface deterioration caused by adsorption processes—at $T = 30$ K on the timescale of only half an hour [37]—both an efficient data acquisition and a fast start of the measurement are essential. The cooling of the sample from the annealing temperature down to $T = 30$ K takes typically 5 min, including the transfer from the preparation chamber to the measurement position on the pre-cooled manipulator.

3. Results on clean surfaces

3.1. Dispersion and Fermi surface of the Shockley state on Au(111)

A grey-scale plot of the photoemission intensity as a function of energy and angle displays directly the dispersion and the splitting of the Au(111) surface state (see figure 2). The dark area around the surface state marks the gap of the projected bulk states, which has its minimum at approximately 1.1 eV, outside the displayed energy range. The occupied part of the two
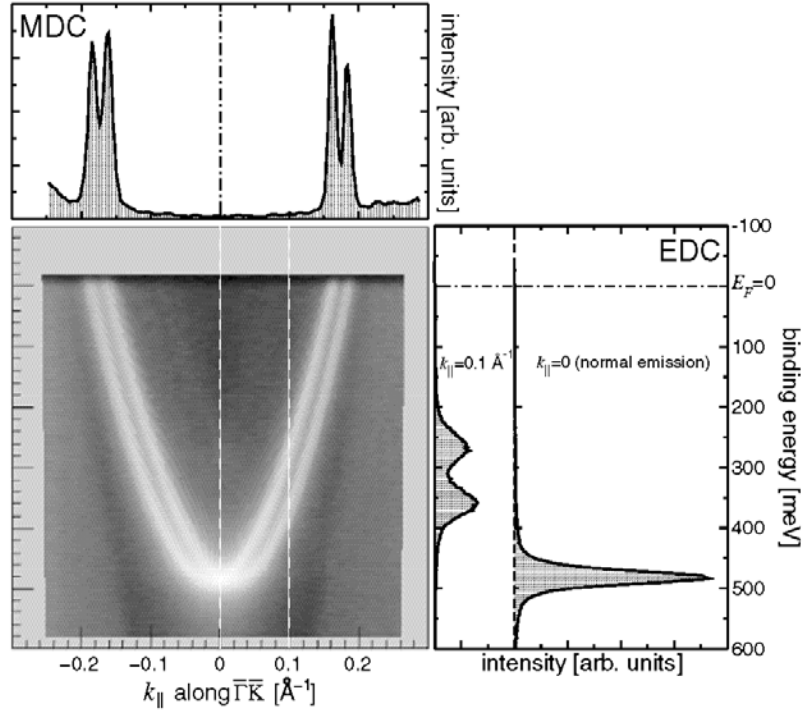
Figure 2. Photoemission intensity of the Shockley state on Au(111) as a function of energy and momentum $I(E_B, k_\parallel)$ (white means high intensity). The top panel shows a cut at constant energy $E = E_F$ (MDC); the right-hand panel gives the energy distribution curves (EDCs) at $k_\parallel = 0$ and $k_\parallel = 0.1$ Å^{-1}.

bright surface state bands can be described nearly perfectly by a superposition of two identical parabolas with a binding energy maximum of $E_0 = 487$ meV, shifted in positive and negative k-directions from $\bar{\Gamma}$, respectively. This is equivalent to a linear increase of the energy splitting with increasing $k_\parallel$ (note that all energies are binding energies relative to the Fermi level, which are positive by definition):

$$E^\pm = -\frac{\hbar^2}{2m^*}\left(k_\parallel \pm \frac{\Delta k}{2}\right)^2 + E_0. \tag{6}$$

A least-squares fit of the dispersion gives an effective mass of $m^* = 0.25\ 1m_e$ and a splitting of $\Delta k = 0.023$ Å^{-1} [23]. The absolute values of Fermi vectors are $|k_F^-| = 0.162$ Å^{-1} and $|k_F^+| = 0.185$ Å^{-1} for the inner and the outer branches, respectively. These values are small compared to the extension of the SBZ, only approximately 15% of the $\bar{\Gamma}\bar{K}$ distance (cf figure 1). Therefore, the Fermi vector length is—within the experimental errors—constant in all in-plane directions and the Fermi surface of the Au(111) Shockley state consists of two concentric cylinders with opposite spin orientations. Figure 3 shows a so-called Fermi surface map (FSM), i.e. the photoemission intensity at E_F as a function of $\mathbf{k}_\parallel = (k_x, k_y)$. This gives the crossing points of the (surface state) bands with the Fermi level in k space. As predicted, one observes two concentric rings, embedded in the dark circular area, representing the projected 'neck' of the bulk Fermi surface, which is characteristic of noble metals [38]. For copper and silver only a single circular Fermi surface for the equivalent Shockley states has been observed [23].
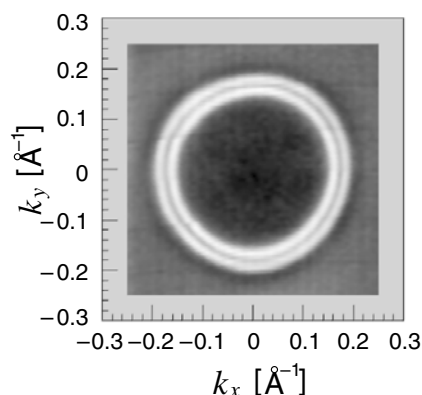
Figure 3. Two-dimensional FSM on Au(111). The two concentric rings represent the spin–orbit split Fermi surface of the Shockley-type surface state, embedded in the projected 'neck' (*L*-gap) of the bulk states. The deviations from a perfect circular shape are due to experimental effects.

3.2. Comparison with band-structure calculations

In principle, the band structure of a surface state can be calculated in the same way as for the bulk states by numerical methods based on the density functional theory (DFT). Here, the perfect three-dimensional solid is described by a infinite periodic repetition of the unit cell. The lack of translational symmetry of a semi-infinite crystal can be recovered by the construction of a super-cell which includes a *slab* of several atomic layers with the atomic order of the crystal [39]. The surface of the crystal is represented by the two surfaces of the slab. The definition of the super-cell includes a certain thickness of vacuum which separates neighbouring slabs in the infinite periodic 'super-crystal'.

An artifact of the slab-layer method is a splitting of the calculated surface states due to a surface–surface interaction through the slab and—but less strong—through the vacuum region. This splitting can be interpreted as the difference in energy between the bonding and anti-bonding overlaps of the respective orbitals of the surface atoms. This artificial splitting can be large compared to a possible spin–orbit splitting when the number of atomic layers in the slab is small. For the investigation of the spin–orbit interaction, the influence of this artefact must be controlled carefully by a variation of the slab distance and thickness.

Figure 4 shows the experimental data from figure 2 together with the results [34] from calculations using the full-potential linearized-augmented-plane wave (LAPW) method in the local density approximation (LDA), embodied in the WIEN97 code [40]. The surface was modelled by a 23-layer slab and a vacuum thickness of 20 bohr (1 bohr = 0.5292 Å), resulting in a spurious surface–surface splitting of about 1 meV which is negligible compared to the spin–orbit splitting of the Shockley state on Au(111). These *ab initio* calculations contain no external parameter to describe the spin–orbit interaction and yield quantitative results for the spin–orbit splitting over the complete investigated k range.

The complete theoretical band structure in figure 4 (solid lines) was shifted by approximately 110 meV to higher binding energies to match the experimental surface state band minimum at $k_\parallel = 0$. Apart from this shift—in other words the position of the Fermi level—the numerical results are in striking agreement with the experiment. Even quantitatively, the band dispersion and the size of the surface state splitting Δk describes nearly perfectly the results from the photoemission experiment. In addition, the position of the bulk band closest to the surface state (dotted) matches nicely the boundary of the projected *L*-gap.
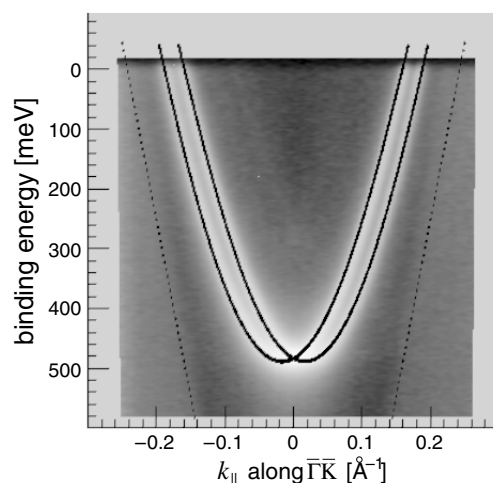
Figure 4. Comparison of the theoretical results (lines) of a 23-layer slab calculation on Au(111) with the experimental data from figure 2. The surface state bands are given as solid lines; the dotted line indicates the dispersion of the bulk band closest to the L-gap (cf figure 7).
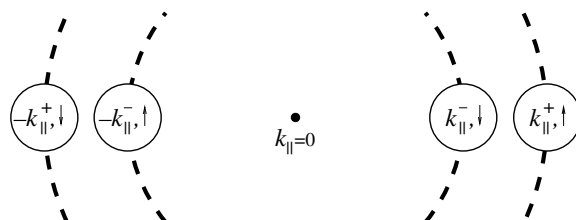

Figure 5. Schematic view of the states involved in the formation of a standing wave at a step edge. The dashed lines indicate lines of constant energy (cf the Fermi surface in figure 3).

It should be mentioned that in contrast to all other face-centred cubic metals the (111) surface of Au is reconstructed. The surface atoms densify along one of the three $\langle \bar{1}10 \rangle$ directions, resulting in a $(22 \times \sqrt{3})$ surface unit cell. Due to elastic stress in the outermost surface layer there is a regular alternation of domains of two orientations, forming the characteristic *herringbone pattern* with a domain width of $\approx$150 Å [32]. This reconstruction was not included in the calculations, since the super-cell size would have been too large to be handled with a reasonable computing time. However, there is some influence of the reconstruction on the electronic properties of the surface, as was observed in STM investigations [41]. But also the photoemission data show indications of the electronic super-lattice at the surface. One can observe the back-folded bands, their contribution to the FSMs and the reduced density of states at the crossing points [42]. The spectral intensity of these back-scattered states is less than 1% of the original surface state and therefore cannot be resolved in figures 2 and 3.

3.3. Experimental information from STM experiments

Scattering of the surface state electrons at defects and step edges leads to the formation of standing wave patterns, which can be observed in STM images at low bias voltages [25, 43].
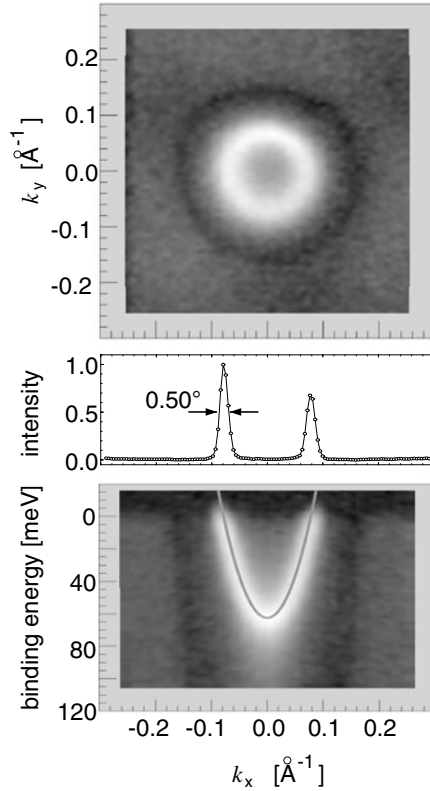
Figure 6. Photoemission results of the equivalent surface state on Ag(111). Top panel, FSM; middle panel, intensity at E_F versus k_x (MDC); lower panel, grey scale plot of the surface state dispersion, including the theoretical results (solid line) from figure 7.

The wavelength of these oscillations is dependent on the bias voltage and can be used to reconstruct the dispersion $E(k)$ of the surface state bands [19, 25, 26]. However, the spin–orbit splitting on Au(111) has never been observed in STM experiments.

An explanation, based on a simple scattering approach, was given by Petersen and Hedegård previously [33]. Simplistically, one can consider the one-dimensional case with an electron of e.g. the right-hand outer branch (labelled with $k_\parallel^+$, ↑ in figure 5) travelling perpendicularly towards a step edge. If we assume that this electron has the wavenumber $k_\parallel^+$, then the reflected electron has the wavenumber $-k_\parallel^+$ but—since no spin-flip can occur—still the same spin direction. Therefore, the two states are orthogonal and cannot interfere to a standing wave pattern. But the spin direction of the reflected electron is identical with the spin direction of the states of the inner left branch with $-k_\parallel^-$. The interference of these to waves leads to a standing wave with $q = k_\parallel^+ + k_\parallel^-$. The same is valid for the other spin direction. Thus, there is only one standing wave type and the information about the k-splitting is lost.

3.4. Other noble metal surfaces

In principle, the equivalent Shockley states on other noble metal surfaces should also show a spin–orbit splitting, but this has never been observed experimentally until now. To get a first estimate about the size of the spin–orbit splitting it is straightforward to compare the $p_{3/2}$–$p_{1/2}$
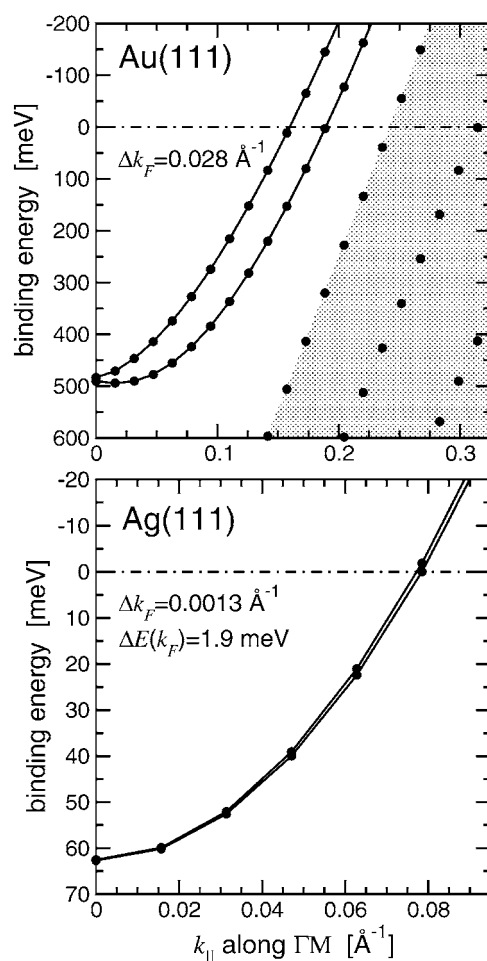
Figure 7. Results of the band-structure calculation along the $\overline{\Gamma}\overline{M}$ direction for a 23-layer slab. Upper panel, the calculated k-splitting for Au(111) amounts to $\Delta k = 0.028$ Å^{-1}. The shaded area represents the projected bulk states. Lower panel, the calculated splitting of the Shockley state is only $\Delta k = 0.0013$ Å^{-1} in momentum, equivalent to an angular splitting of $\Delta\theta = 0.035°$ at He I.

splittings of the considered p states of a free atom [44], which amount to 470, 110 and 31 meV for Au 6p, Ag 5p and Cu 3p, respectively. In the case of Cu the atomic value is a factor of 15 smaller than for Au, and thus the splitting is beyond the experimental resolution. But in principle, a splitting which is only a factor of four smaller than for Au should leave its mark in the high-resolution photoemission data. However, the experimental data on Ag(111) do not show a split surface state (see figure 6). This discrepancy again can be examined by the comparison of the experiment with band-structure calculations. Figure 7 shows the numerical results of a 23-layer slab calculation for Ag(111) and Au(111). Obviously, the k-splitting for Ag is much smaller than the estimate from the atomic parameters: Δk is only 0.0013 Å^{-1} at the Fermi level, equivalent to an angular splitting of 0.035° at the used photon energy, one order of magnitude below the angular resolution $\Delta\theta \approx 0.3°$ of the experimental setup.
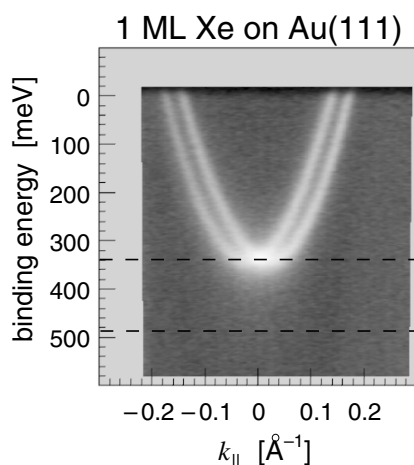
1 ML Xe on Au(111)

Figure 8. Dispersion of the Shockley state on Au(111) covered with one monolayer of xenon (after an exposure of 4.7 L, $T = 65$ K, see [37]). The surface state is shifted towards the Fermi level and reveals an increased spin–orbit splitting of $\Delta k = 0.031$ Å^{-1}. The horizontal dashed lines indicate the binding energy of the band minimum E_0 of the clean and the covered surface.

There are mainly two factors that determine the size of the splitting of the surface state:

(1) the gradient of the crystal potential $V(r)$ perpendicular to the surface, and
(2) the amount of p character in the sp surface state.

A detailed understanding of these factors requires extended DFT calculations and a closer look at the resulting wavefunctions.

3.5. Adsorbate covered surfaces

An interesting modification of the surface state on Au(111) can be observed when the surface is covered by a closed monolayer of a rare gas. As displayed in figure 8 for Xe on Au(111), the most obvious effect is a shift of the surface state bands towards the Fermi level, which can be explained by a Pauli repulsion between the closed-shell electrons from the adsorbate and the wavefunction of the surface state [45]. The size of the shift depends on the 'nobleness' of the rare gas and thus increases with the periodic number [46, 47]. In addition, there is an increase of the spin–orbit splitting Δk by about 30%, which possibly can be explained by the Pauli repulsion as well. The Pauli repulsion experienced by the surface state electrons can be described as an additional repulsive potential close to the surface, that also increases the steepness—i.e. the gradient—of the net potential $V(r)$ perpendicular to the surface. According to equation (5) the spin–orbit interaction increases and leads to a larger splitting of the surface state bands.

4. Conclusions

This paper presents a summary of recent high-resolution photoemission investigations on the Shockley-type surface state on the (111)-face of gold. To date this surface is the only noble metal surface that shows a considerable splitting of the surface state, which unambiguously can be explained by spin–orbit interaction in the sp states as first suggested by LaShell, McDougall and Jensen. The characteristic herringbone reconstruction on Au(111) has only a comparatively

small influence on the photoemission data and is negligible in the discussion of the spin–orbit splitting. Fully relativistic band-structure calculation show an excellent agreement with the experimental results and can quantitatively describe the splitting, which for other noble metal surfaces is too small to be experimentally observed. A more extended numerical analysis will include calculations on adsorbate covered surfaces, which might give interesting information about the electronic interface properties of the system.

Acknowledgments

References

[1] Tamm I E 1932 On the possible bound states of electrons on a crystal surface *Phys. Z. Sowjet.* **1** 733
[2] Shockley W 1939 On the surface states associated with a periodic potential *Phys. Rev.* **56** 317–23
[3] Davison S G and Stęślicka M 1992 *Basic Theory of Surface States* (Oxford: Oxford University Press)
[4] Bertel E and Donath M (ed) 1994 *Electronic Surface and Interface States on Metallic Systems* (Singapore: World Scientific)
[5] Gartland P O and Slagsvold B J 1975 Transition conserving parallel momentum in photoemission from the (111) face of copper *Phys. Rev.* B **12** 4047–58
[6] Heimann P, Neddermeyer H and Roloff H F 1977 Ultraviolet photoemission from intrinsic surface states of the noble metals *J. Phys. C: Solid State Phys.* **10** L17–21
[7] Kevan S D 1983 Evidence for a new broadening mechanism in angle-resolved photoemission from Cu(111) *Phys. Rev. Lett.* **50** 526–9
[8] Kevan S D 1986 Direct measure of surface impurity scattering by angle-resolved photoemission *Phys. Rev.* B **33** 4364–6
[9] Matzdorf R and Goldmann A 1996 High-resolution photoemission study of the $\bar{M}$-surface states on Cu(111) *Surf. Sci.* **359** 77–81
[10] Beckmann A, Meinel K, Ammer Ch, Heiler M and Neddermeyer H 1997 Asymmetric peak broadening in photoemission of surface states as a consequence of lateral electron confinement *Surf. Sci.* **375** L363–6
[11] McDougall B A, Balasubramanian T and Jensen E 1995 Phonon contribution to quasiparticle lifetimes in Cu measured by angle-resolved photoemission *Phys. Rev.* B **51** 13891
[12] Paniago R, Matzdorf R, Meister G and Goldmann A 1995 Temperature dependence of Shockley-type surface energy bands on Cu(111), Ag(111) and Au(111) *Surf. Sci.* **336** 113–22
[13] Balasubramanian T, Jensen E, Wu X L and Hulpert S L 1998 Large value of the electron–phonon coupling parameter ($\lambda = 1.15$) and the possibility of surface superconductivity at the Be(0001) surface *Phys. Rev.* B **57** R6866–9
[14] Hengsberger M, Purdie D, Segovia P, Garnier M and Baer Y 1999 Photoemission study of a strongly coupled electron–phonon system *Phys. Rev. Lett.* **83** 592–5
[15] Hengsberger M, Frésard R, Purdie D, Segovia P and Baer Y 1999 Electron–phonon coupling in photoemission spectra *Phys. Rev.* B **60** 10796–802
[16] Valla T, Fedorov A V, Johnson P D and Hubert S L 1999 Many-body effects in angle-resolved photoemission: quasiparticle energy and lifetime of a Mo(110) surface state *Phys. Rev. Lett.* **83** 2085–8
[17] LaShell S, Jensen E and Balasubramanian T 2000 Nonquasiparticle structure in the photoemission spectra from the Be(0001) surface and determination of the electron self energy *Phys. Rev.* B **61** 2371–4
[18] Rotenberg E, Schaefer J and Kevan S D 2000 Coupling between adsorbate vibrations and an electronic surface state *Phys. Rev. Lett.* **84** 2925–8
[19] Li J, Schneider W-D and Berndt R 1997 Local density of states from spectroscopic scanning-tunneling-microscope images: Ag(111) *Phys. Rev.* B **56** 7656–9

[20] Li J, Schneider W-D, Berndt R, Bryant O R and Crampin S 1998 Surface state lifetime measured by scanning tunneling spectroscopy *Phys. Rev. Lett.* **81** 4464–7

[21] Berndt R, Schneider W-D and Crampin S 1999 Surface-state linewidth from scanning tunnelling spectroscopy *Appl. Phys.* A **69** 503–6

[22] Kliewer J, Berndt R, Chulkov E V, Silkin V M, Echenique P M and Crampin S 2000 Dimensionality effects in the lifetime of surface states *Science* **288** 1399–402

[23] Reinert F, Nicolay G, Schmidt S, Ehm D and Hüfner S 2001 Direct measurements of the *L*-gap surface states on the (111) face of noble metals by photoelectron spectroscopy *Phys. Rev.* B **63** 115415

[24] Echenique P M, Pitarke J M, Chulkov E V and Rubio A 2000 Theory of inelastic lifetimes of low-energy electrons in metals *Chem. Phys.* **251** 1–35

[25] Crommie M F, Lutz C P and Eigler D M 1993 Imaging standing waves in a two-dimensional electron gas *Nature* **363** 524–7

[26] Bürgi L, Petersen L, Brune H and Kern K 2000 Noble metal surface states: deviations from parabolic dispersion *Surf. Sci.* **447** L157–61

[27] Hüfner S 1996 *Photoelectron Spectroscopy (Springer Series in Solid-State Sciences vol 82)* (Berlin: Springer)

[28] LaShell S, McDougall B A and Jensen E 1996 Spin splitting of an Au(111) surface state band observed with angle resolved photoelectron spectroscopy *Phys. Rev. Lett.* **77** 3419–22

[29] Petersen L, Laitenberger P, Lægsgaard E and Besenbacher F 1998 Screening waves from steps and defects on Cu(111) and Au(111) imaged with STM: contribution from bulk electrons *Phys. Rev.* B **58** 7361–6

[30] Fujita D, Amemiya K, Yakabe T, Nejoh H, Sato T and Iwatsuki M 1999 Observation of a two-dimensional Fermi contour of a reconstructed Au(111) surface using Fourier transform scanning tunneling microscopy *Surf. Sci.* **423** 160–8

[31] Petersen L, Bürgi L, Brune H, Besenbacher F and Kern K 1999 Comment on 'Observation of a two-dimensional Fermi contour of a reconstructed Au(111) surface using Fourier transform scanning tunneling microscopy' by D Fujita *et al* 1999 *Surf. Sci* **423** 160 *Surf. Sci.* **443** 154–6

[32] Narasimhan S and Vanderbilt D 1992 Elastic stress domains and the herringbone reconstruction on Au(111) *Phys. Rev. Lett.* **69** 1564–7

[33] Petersen L and Hedegård P 2000 A simple tight-binding model of spin–orbit splitting of sp-derived surface states *Surf. Sci.* **459** 49–56

[34] Nicolay G, Reinert F, Hüfner S and Blaha P 2002 Spin–orbit splitting of the *L*-gap surface state on Au(111) and Ag(111) *Phys. Rev.* B **65** 033407

[35] Eiguren A, Hellsing B, Reinert F, Nicolay G, Chulkov E V, Silkin V M, Hüfner S and Echenique P M 2002 Role of bulk and surface phonons in the decay of metal surface states *Phys. Rev. Lett.* **88** 066805

[36] Nicolay G, Reinert F, Schmidt S, Ehm D, Steiner P and Hüfner S 2000 Natural linewidth of the Ag(111) L-gap surface state as determined by photoemission spectroscopy *Phys. Rev.* B **62** 1631–4

[37] Nicolay G, Reinert F, Forster F, Ehm D, Schmidt S, Eltner B and Hüfner S 2002 About the stability of noble metal surface states during VUV-experiments *Surf. Sci.* submitted

[38] Ashcroft N W and Mermin N D 1988 *Solid State Physics* (Philadelphia, PA: Saunders)

[39] Springborg M 2000 *Methods of Electronic-Structure Calculations: From Molecules to Solids (Wiley Series in Theoretical Chemistry)* (New York: Wiley)

[40] Blaha P, Schwarz K and Luitz J 1999 *WIEN97, A Full Potential Linearized Augmented Plane Wave Package for Calculating Crystal Properties* Technical University of Vienna (ISBN 3-9501031-0-4)
This is an improved and updated Unix version of the original copyrighted WIEN code, which was published by Blaha P, Schwarz K, Sorantin P and Trickey S B 1990 *Comput. Phys. Commun.* **59** 399

[41] Chen W, Madhavan V, Jamneala T and Crommie M F 1998 Scanning tunnelling microscopy observation of an electronic superlattice at the surface of clean gold *Phys. Rev. Lett.* **80** 1469–72

[42] Nicolay G 2002 Untersuchungen zur elektronischen Struktur *in situ*-präparierter Edelmetalloberflächen *PhD Thesis* Universität des Saarlandes

[43] Hasegawa Y and Avouris Ph 1993 Direct observation of standing wave formation at surface steps using scanning tunneling spectroscopy *Phys. Rev. Lett.* **71** 1071–4

[44] Moore C E 1949, 1952 *Atomic Energy Levels* NBS Circular no 467, vols 2 and 3 (Washington, DC: US Government Printing Office)

[45] Bertel E and Memmel N 1996 Promotors, poisons and surfactants: electronic effects of surface doping on metals *Appl. Phys.* A **63** 523–31

[46] Hövel H, Grimm B and Reihl B 2001 Modification of the Shockley-type surface state on Ag(111) by an adsorbated xenon layer *Surf. Sci.* **477** 43–9

[47] Forster F, Nicolay G, Reinert F, Ehm D and Hüfner S 2002 Interface and surface states on adsorbate covered noble metal surfaces *Surf. Sci.* at press